ELSEVIER

Ecological Modelling 102 (1997) 259–272

ECOLOGICAL MODELLING

Long term simulations of population dynamics of *Ulva r.* in the lagoon of Venice

C. Solidoro *, V.E. Brando, C. Dejak, D. Franco, R. Pastres, G. Pecenik

Department of Physical Chemistry, Section of Ecological Physical Chemistry, University of Venice, Dorsoduro 2137, Venice 30123, Italy

Accepted 13 March 1997

Abstract

The dynamic of macroalgae is implemented in a 3D transport-water-quality model of the central part of the lagoon of Venice. Ulva biomass density and nitrogen concentration in Ulva tissue have been added to the set of state variables previously considered, that is to phytoplankton and zooplankton densities, concentrations of nutrients in water, detritus and dissolved oxygen. The model shows that Ulva succeeds in the competition with the phytoplanktonic community in the shallower areas, where water temperature and irradiance levels reaching the bottom are sufficient to sustain growth. Long term evolutions of Ulva colonies, under different scenarios of forcing functions, show that adverse meteoclimatic conditions can be more effective in reducing Ulva biomass than a consistent decrease in the loads of Nitrogen. © 1997 Elsevier Science B.V.

Keywords: Water quality; Macroalgae; Competition; 3D model; Venice

1. Introduction

In the early eighties, the macroalgae community became an important component of the ecosystem in the Venice lagoon, reaching standing crops at an order of magnitude higher than those of the phytoplanktonic pool in 1987 and 1989. High levels of biomass production have been maintained from early spring to late autumn in large areas of the lagoon, with biomass density of up to about 20 kg/m^2 (wet weight). Under particular conditions, anoxic crises are likely to occur, especially during the summer, followed by sharp collapses in population, and resultant releases of hydrogen sulphide (Sfriso et al., 1987, 1989). The massive presence of *Ulva rigida*, by far the most dominant species (Sfriso, 1987), has heavily affected the ecosystem, and has prompted new field and model studies, aimed at understanding the

* Corresponding author. Fax: + 39 41 5298594; e-mail: cosimo@unive.it

PII S0304-3800(97)00060-4

reasons for such a change and at forecasting the long-term evolution of the system.

A few models of the dynamic of *Ulva r* have already been proposed, both zero dimensional (Bendoricchio et al., 1994; Pecenik et al., 1991) and one dimensional (Solidoro et al., 1997b), but a full understanding of the seasonal cycle of macroalgae and of the mechanisms underlying the behaviour of the ecosystem requires the development of a 3D model. In fact, only in this way one can describe the transport phenomena and the interactions between biotic and abiotic components, as well as the competition with other communities, such as that of phytoplankton. This paper presents the implementation of *Ulva r*. dynamic (Solidoro et al., 1997b) in a 3D model (Dejak and Pecenik, 1987), whose major features are briefly outlined below.

2. General features of the 3D model

The 3D finite-difference model covers the central part of the lagoon of Venice and includes the most important industrial area and the city of Venice. This area is divided on a mesh of 100 m by 100 m, with a vertical step of 1 m, in order to reproduce the bathometry in sufficient detail (Fig. 1). The model, developed during the eighties, couples transport processes with the dynamics of the communities of primary producers and that of zooplankton (Dejak and Pecenik, 1987; Dejak et al., 1990), and succeeds in simulating the seasonal evolution of the lower trophic levels. The dynamic of the dissolved oxygen concentration is also included, as it is an important water quality index.

Advective terms are not considered (Dejak et al., 1987a), because of the marginal influence of the residual current in this water body. As a consequence, the average effect of tidal agitation has been embodied in the turbulent diffusion. Eddy diffusion coefficients are the same for all species, but they are not constant throughout the spatial domain. The horizontal diffusivities have been estimated on the basis of a statistical approach, as in Dejak et al. (1995). Along the vertical column, eddy diffusivities have been calibrated by comparing the model output with many temperature profiles observed in the deepest channels (Dejak et al., 1992). Open boundary conditions are discussed in (Dejak et al., 1987b).

After the inclusion of *Ulva r*. dynamics (Solidoro et al., 1995), the model follows the evolution of eleven state variables: zooplankton (Z), phytoplankton (P) and *Ulva r*. (U) density; internal nitrogen in *Ulva r*., quota, (Q), concentrations of NH_4^+, NO_3^- and PO_4^{3-} in the water, nitrogen as detritus, (DN), nitrogen in the sediment, (SN), and dissolved oxygen (DO).

Temperature, T, is considered as a state variable, because it varies within the spatial domain. Its seasonal evolution is forced by solar radiation and heat exchanges with the atmosphere (Dejak et al., 1992). Local perturbations, due to the presence of a power plant, are also taken into account. Heat diffusion within the water body is treated in the same way as the diffusion of the other state variables.

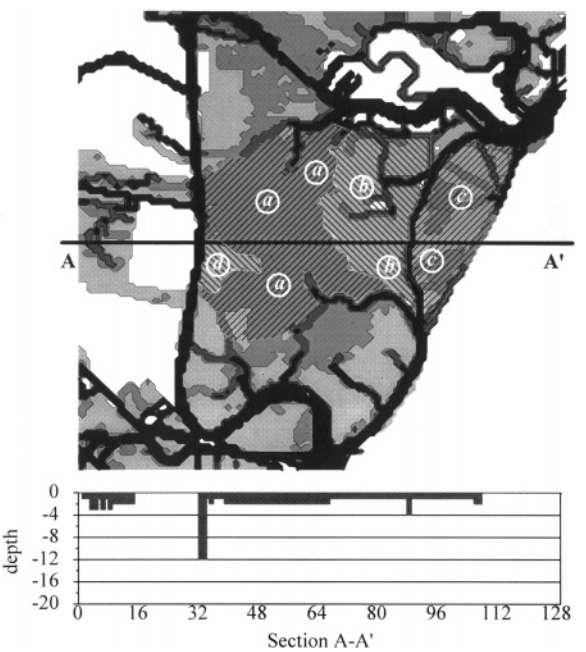

Fig. 1. Area covered by the model and depth along the section A-A′. Gray intensity increases with depth. Superimposed pattern and encircled letters mark the areas *a*, *b*, *c* and *d*. Areas *b* and *d* are mostly 1 m deep, area *a* 2 m deep, while area *c* contains both 1 and 2 m deep regions. Areas *b* and *c* are physically separated by a 4 m deep channel.

The nutrients loads are, together with energetic inputs, forcing functions for the model. The loads have been estimated on the basis of the available data (CVN, 1993); immission points are shown in Fig. 1.

The reaction–diffusion equation is solved by a fractional step method, that is by decomposing the 3D problem in three 1D ones. The integration is carried out by using an implicit method, (Dejak et al., 1987a,b), which guarantees stability and conservativity at high diffusion numbers. The method has been efficiently implemented, also in the exploitation of the potentialities of vector parallel supercomputer (Pastres et al., 1995), but, at present, the model can also be run on medium-size workstations.

3. Major features of the trophic submodel

The formulations here proposed, Table 1, take into account the characteristics of two communities of primary producers, phytoplankton and macroalgae. The governing equations for the two groups will be briefly discussed together, in order to highlight their similarities and differences. Formulations concerning the dynamics of Ulva and their experimental basis are discussed in detail in Solidoro et al. (1997b).

Phytoplanktonic species are pooled, and the composition of the pool in terms of major chemicals is kept constant (Redfield, 1934). This implies that the cells are in a steady-state condition and, therefore, the processes of growth and assimilation of nutrients from the water column are described by a single step kinetic. On the contrary, experimental evidence (Cohen and Neori, 1991; Fujita, 1985) indicates as more appropriate a distinction between assimilation and growth for *Ulva r*., because macroalgae store the excess of Nitrogen and use it for maintaining their metabolic efficiency when the concentration of Nitrogen in the water body is low. Internal storage plays a key role in regulating both growth rate, that does not depend on the external concentration of nitrogen, Eq. (14), and uptake rates, which are inversely related to storage, and proportional to external concentration, Eq. (12), Eq. (13).

The influence of limiting factors is accounted for in a multiplicative formulation for both communities, Eqs. (14) and (24), (Joergensen, 1988). A Monod-type kinetic describes the limitation of phytoplankton growth and macroalgae uptake, due to the lack of nitrogen Eqs. (28), (12) and (13), and phosphorus, Eqs. (29) and (18). The two groups assimilate nutrients in accordance with their own kinetic, as there is no a priori definition of a competitive efficiency. In this way, rates of uptake vary with local conditions, and microalgae and *Ulva r*. compete for nutrients when their concentrations are low.

The dependence of phytoplankton growth on water temperature is modelled by a Lassiter–Kearns function, Eq. (27), whereas a sigmoidal function has been chosen for macroalgae, Eq. (20). The influence of light is described by a Steel function for phytoplankton, Eq. (25), while an asymptotic formulation has been adopted for the other community, Eq. (15). Other formulations, which consider inhibition phenomena at high irradiance values, can be found in literature (Bendoricchio et al., 1993), but they require the estimation of a greater number of parameters. However, they would be in close agreement with the formulations here proposed, within the range of irradiance commonly found in the lagoon of Venice.

Incident light at the surface is interpolated from averaged monthly values, and its attenuation along the water column is computed according to a discretization of the Lambert–Beer law. Phytoplankton is affected only by self-shading, Eq. (26), as its presence is greater in the upper layers, while *Ulva r*., being in the deepest layers, is shaded by phytoplankton and by itself, Eq. (19).

Oxygen availability is another factor in competition. For both phytoplankton and macroalgae, the respiration rate is a linear function of the density, but the temperature dependence is different, being exponential for phytoplankton, Eq. (2), and asymptotical for Ulva, Eq. (20). In the model here proposed, a negative feedback relates the mortality rate of *Ulva r*. with the concentration of DO. The increase in mortality rate is proportional to the difference between the oxygen demand exerted by respiration, and the availability of DO, Eq. (3), that is, to the fraction of biomass that can not respire and is likely to be damaged.

Table 1
State variables and state equations of the model and functional forms used in the model

Global model

State variables

Z	density of zooplankton	mgC/l
P	density of phytoplankton	mgC/l
U	density of Ulva	gdw/l
Q	quota (nitrogen concentration in Ulva tissue)	mgN/gdw
NH_4^+	water concentration of reduced inorganic nitrogen	mgN/l
NO_x^-	water concentration of oxidized inorganic nitrogen	mgN/l
PO_4^{3-}	water concentration of reactive phosphorous	mgP/l
DN	nitrogen in the detritus	mgN/l
SN	nitrogen in the sediment	mgN/l
DO	water concentration of dissolved oxygen	mgO/l

Equations

$$dZ/dt = \{k_{grz} f(P) Z E_{ff} - K_{mZ} - k_{escZ}\} a(T) Z \quad (1)$$

$$dP/dt = \varphi P - (k_{mP} a(T) + k_{sedP} + k_{rP} a(T)) P - k_{grz} a(T) f(P) Z \quad (2)$$

$$dU/dt = \mu U - K_{mU} U^{\gamma} - k_t \frac{\max[(f_{ru}(T)U - DO), 0]}{f_{ru}(T)U} \quad (3)$$

$$dQ/dt = T_{SU} - \mu Q \quad (4)$$

$$dNH_4^+/dt = -T_{SUNH} U - T_{SPNH} P + k_{nit} a(T) NH_4^+ + R_{NC}\{k_{rP} P + k_{escZ} Z\} a(T) \quad (5)$$

$$dNO_x^-/dt = -T_{SUNO} U - T_{SPNO} P - k_{nit} a(T) NH_4^+ \quad (6)$$

$$dPO_4^{3-}/dt = -R_{UPC} \mu U - R_{PC} \varphi P + R_{PC}\{k_{rP} P + k_{escZ} Z\} a(T) \quad (7)$$

$$dDN/dt = R_{NC}\{k_{mP} a(T) + k_{mZ} a(T) Z + (1 - E_{ff}) k_{grz} f(P) Z\} - (k_{dec} + k_{sed}) DN + k_{mU} Q + Q k_t \frac{\max[f_{ru}(T)U - DO), O]}{f_{ru}(T)U} \quad (8)$$

$$dSN/dt = k_{sed} DN - k_{dec} SN a(T) \quad (9)$$

Table 1 (continued)

Global model

$$dDO/dt = [\psi\mu - k_{rU} f_{ru}(T)] U + R_{OC}[\phi - k_{rP}] P - R_{nit} k_{nit} NH_4^+ - R_{ON} k_{decn}(DN + SN) a(T) + k_{rear}(DO_{sat} - DO) \quad (10)$$

Functional forms used in the macroalgae model

$$T_{SU} = T_{SUNH} + T_{SUNO} \quad (11)$$

$$T_{SUNH} = [V_{NH} NH_4^+/(NH_4^+ + k_{NH})] [(Q_{max} - Q)/(Q_{max} - Q_{min})] \quad (12)$$

$$T_{SUNO} = [V_{NO} NO_x^-/(NO_x^- + k_{NO})] [(Q_{max} - Q)/(Q_{max} - Q_{min})] \quad (13)$$

$$\mu = \mu_{max} f_u(I) f_u(T) f_u(Q) f_u(PO_4^{3-}) \quad (14)$$

$$f_u(I) = 1 - \exp(-I_i/I_S) \quad (15)$$

$$f_u(T) = \left\{\frac{1}{[1 + \exp(-\zeta(T - \vartheta))]}\right\} \quad (16)$$

$$f_u(Q) = (Q - Q_{min})/(Q - k_{lc}) \quad (17)$$

$$f_u(PO_4^{3-}) = PO_4^{3-}/(PO_4^{3-} + k_{up}) \quad (18)$$

$$I_i = I \exp\{\epsilon_P[P(z-1) + \cdots + P(1)] + \epsilon_u[B(z-1) + \cdots + B(1)] + \epsilon_w\} \quad (19)$$

$$f_{ru}(T) = \left\{\frac{1}{[1 + \exp(-\zeta_r(T - \vartheta_r))]}\right\} \quad (20)$$

Functional forms used in the phytoplankton model

$$T_{SPNH} = R_{NC}\left(\frac{NH_4^+}{N_{tot}}\right)\varphi \quad (21)$$

$$T_{SPNO} = R_{NC}\left(\frac{NO_x^-}{N_{tot}}\right)\varphi \quad (22)$$

$$f(P) = \frac{P}{(P + k_{pZ})} \quad (23)$$

$$\varphi = \varphi_{max} f(I) f(T) f(N) f(PO_4^{3-}) \quad (24)$$

$$f(I) = e/\alpha_1\{\exp[-\alpha_2 \exp(-\alpha_1)] - \exp(-\alpha_2)\} \quad (25)$$

Table 1 (continued)

Global model

$$\alpha_1 = k_h z \quad \alpha_2 = \frac{I}{I_{oP}} k_h \tag{26}$$

$$k_h = \epsilon_P \{0.5P(z) + P(z-1) + \cdots + P(1)\}$$

$$f(T) = [(T_a - T)/(T_a - T_o)]^{a(T_a - T_o)\exp[a(T_a - T_a)]} \tag{27}$$

$$f(N) = N_{tot}/(N_{tot} + k_{Pn}) \tag{28}$$

$$f(PO_4^{3-}) = PO_4^{3-}/(PO_4^{3-} + k_{Pp}) \tag{29}$$

$$DO_{sat} = 14.6244 - 0.367134T + 0.0044972T^2 - 0.0966S + 0.00005TS + 0.0002739S^2 \tag{30}$$

$$N_{tot} = NH_4^+ + NO_x^- \tag{31}$$

$$a(T) = 1.07^{(T-20)} \tag{32}$$

The intrinsic mortality is linear for phytoplankton, Eq. (2), but is proportional to U^γ for the other community, Eq. (3). Phytoplankton is grazed by zooplankton, following a type II functional response, Eq. (23), while the predation of macroalgae has not been explicitly considered, given the lack of quantitative data.

Phytoplankton is treated as a passive tracer, but this hypothesis can not be applied to Ulva, due to its size. The residual currents have been found to be preferential paths for the expansion of the colonies of macroalgae (Menesguem and Salomon, 1987). Nevertheless, no quantitative information on this process is available for the lagoon of Venice, where residual currents, as has already been remarked, are negligible. Therefore, Ulva is assumed to spread according to an isotrophic diffusion process. The diffusion coefficient is a constant, which has been determined by comparing observed and computed distributions, (Solidoro et al., 1996a).

All loss terms are transferred to the detritus component, DN, which is defined as the labile fraction of organic matter which can be mineralized, consumes oxygen and releases nutrients back into the water medium. Detritus sedimentates at a constant rate, and is transeferred to the surface sediment, SN, when it reaches the bottom. The specific rates of mineralization of SN and DN depend on the concentration of DO, because the bacterial activity is assumed to be in a steady state condition (Voinov and Tonkikh, 1987), Eq. (30).

The parameters listed in Table 2 have been estimated on the basis of a thorough analysis of functional measurements collected for the purpose, and of a critical comparison of suggestions made in literature, whenever local experimental findings were not available (Bertonati et al., 1987; CRTSF, 1989, 1994; Solidoro et al., 1997b).

The formulations and their parameterization have been tested by analysing the behaviour of a single water column, which can exchange oxygen and energy with the atmosphere, but does not receive an input of nutrients. This represents a 1D version of the model, in which Nitrogen and Phosphorous, which are rapidly recycled by the process of mineralization, are conserved. The yearly dynamic of this model shows either the extinction of one community or a seasonal succession of blooms of *Ulva r.* and phytoplankton. Even though the two communities compete for the available nutrients, their coexistence, or their extinction, is mainly regulated by the physical factors connected with light intensity, such as the depth of the water column and shading coefficients, and their photosynthetic efficiencies, I_{oP}, I_s. The key role of the above parameters has been confirmed by a systematic local sensitivity analysis around the nominal values of all the parameters (Solidoro et al., 1996b; Pastres et al., 1997).

An example of the cyclic coexistence of phytoplankton and macroalgae is shown in Fig. 2a, while Fig. 2b displays a non-periodical evolution, obtained by modifying the shading coefficients; examples of both patterns can be observed in the lagoon of Venice. Phytoplankton blooms are shorter and more intense than macroalgae ones, and they occur before the first macroalgae bloom and after the major macroalgae collapse. A comparative analysis of a whole set of simulations shows that the phytoplankton dynamic is sensitive to changes in external environmental conditions, whereas macroalgae evolution is less affected by external factors, because of the presence of inter-

Table 2
Parameters used in the model

Parameters for Ulva		
$\mu_{max} = 0.45$	max specific growth rate	(d^{-1})
$k_{lc} = 7$	critical N quota level	(mg N/g dw)
$V_{NH} = 8.5$	max specific uptake rate for ammonium	(mg N/g dw h)
$V_{NO} = 0.45$	max specific uptake rate for nitrate	(mg N/g dw h)
$k_{NH} = 0.1$	half saturation for ammonium	(mg N/l)
$k_{NO} = 0.05$	half saturation for nitrate	(mg N/l)
$Q_{max} = 42$	max value for N quota	(mg N/g dw)
$Q_{min} = 10$	min value for N quota	(mg N/g dw)
$R_{UPC} = 2.5$	stochiometric ratio	(mg P/g dw)
$k_{rU} = 2.54$	max respiration rate	(mg O/g dw h)
$\zeta = 0.2$	temperature coefficient	$°C^{-1}$
$\zeta_r = 0.3$	temperature coefficient	$°C^{-1}$
$\theta = 12.5$	temperature coefficient	°C
$\theta_r = 10$	temperature coefficient	°C
$I_S = 5800$	photosynthetic efficiency parameter	(lux)
$k_{PU} = 0.01$	half saturation for PO_4^{3-}	(mg P/l)
$\epsilon_U = 20$	self-shading coefficient	(g C^{-1})
$k_{mU} = 0.005$	mortality rate	(h^{-1})
$\gamma = 0.84$	coefficient	
$\Psi = 1450$	stochiometric ratio	(mg O_2/g dw)
Parameters for phytoplankton		
$\varphi_{max} = 0.12$	max specific growth rate	(h^{-1})
$k_{Pn} = 0.05$	half-saturation for N	(mg N/l)
$k_{Pp} = 0.01$	half saturation for PO_4^{3-}	(mg P/l)
$T_a = 35$	temperature inhibiton threshold growth	(°C)
$T_o = 31$	optimal temperature for growth	(°C)
$I_{oP} = 50000$	optimal irradiance level growth	(lux)
$\epsilon_P = 0.001$	self-shading coefficients	(g C^{-1})
$k_{rP} = 0.004$	respiration rate	(h^{-1})
$k_{mP} = 0.005$	mortality rate	(h^{-1})
$k_{sedP} = 0.0005$	sedimentation. rate	(m/h)
$R_{NC} = 0.15$	stochiometric ratio	(mg N/mg C)
$R_{PC} = 0.023$	stochiometric ratio	(mg P/mg C)
Parameters for zooplankton		
$k_{grz} = 0.05$	grazing rate	(h^{-1})
$k_{mZ} = 0.005$	mortality rate	(h^{-1})
$E_{ff} = 0.7$	grazing efficiency	
$k_{escZ} = 0.002$	excretion rate	(h^{-1})
$k_{pZ} = 1.0$	half-saturation for grazing	(mg C/l)

Table 2 (continued)

Others Parameters		
$k_{sed} = 0.004$	sedimentation rate	(m/h)
$k_{nit} = 0.0023$	nitrification rate	(h^{-1})
$k_{dec} = 0.0048$	decay rate	(h^{-1})
$k_{rear} = 0.045$	reareation rate	(h^{-1})
$\epsilon_w = 0.4$	water extinction coefficients	(m^{-1})
$S = 30$	average salinity of the Venice lagoon	(PSU)
$R_{nit} = 4.5$	stochiometric ratio	
$R_{ON} = 17.7$	stochiometric ratio	(mg O/mg N)
$R_{OC} = 2.66$	stochiometric ratio	(mg O/mg C)

nal nitrogen storage and of its ability to cope with low irradiance and temperatures. Macroalgae blooms cause marked decreases in the concentrations of nutrients in the whole water column, even though they are present only in the bottom layers. This behaviour, which has not been illustrated here, is due to the rapid mixing of dissolved substances, induced by the diffusion process.

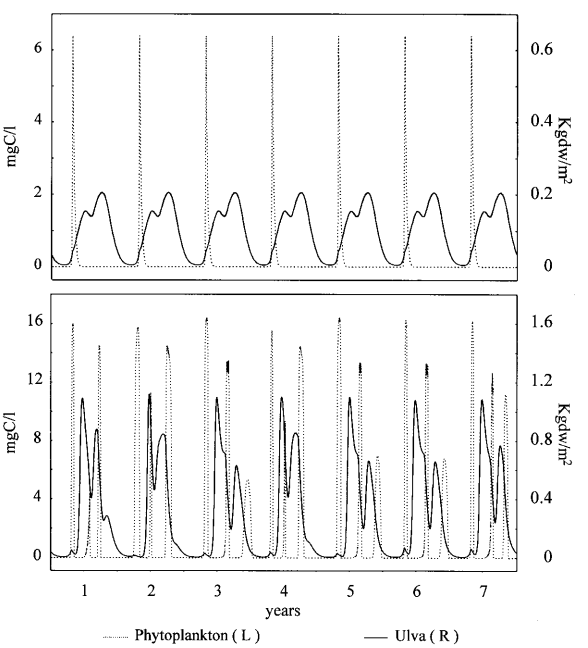

Fig. 2. Time evolution of phytoplankton and macroalgae in simulations obtained with the 1D reaction diffusion model for different value of the shading coefficient.

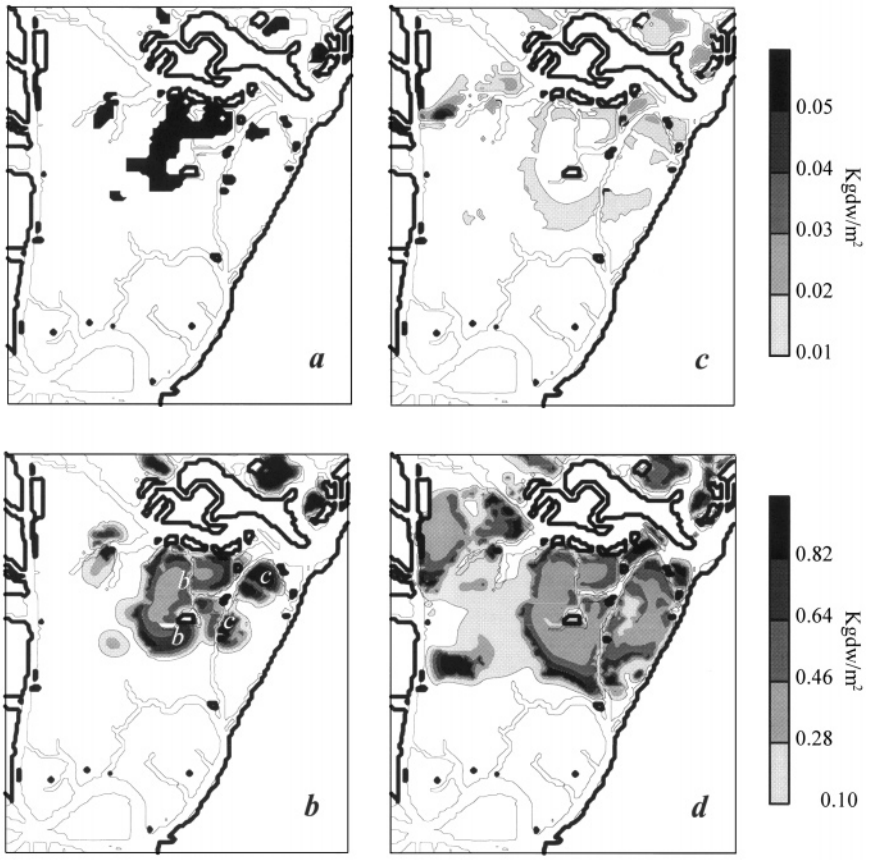

Fig. 3. Initial condition for Ulva as derived from remote sensing image (a), spatial distribution of Ulva density on day 210 of the first year of simulation (b), day 80 of the second year of simulation (c) and day 210 of the second year of simulation (d).

4. Results and discussion

4.1. Analysis of the evolution in the reference scenario of forcing functions

The 3D model allows one to study the ecosystem in realistic conditions of inflows and outflows of nutrients. In a first simulation, the initial density of macroalgae has been taken as a constant for the whole area, in order to check if the model would succeed in giving rise to temporal and spatial patterns. This simulation confirms that Ulva colonies survive only in shallower areas, less than 2 meters deep, whereas the distribution of phytoplankton is not correlated with the bathometry. The spatial distribution of Ulva colonies is explained by the low solar radiation which reaches the bottom below that depth, in an environment characterized by a low transparency.

Spatial distributions closer to the observed ones have been obtained by assigning the initial condition for Ulva on the basis of a remote sensing image: initial Ulva density has been set to a constant value in the black area of Fig. 3a, and zero elsewhere (Solidoro et al., 1996a). Initial conditions have a considerable influence on the spatial distribution, but do not modify the essential features of the seasonal evolution. The model has been run for two consecutive years, using the same yearly scenario of nutrient inputs and meteoclimatic conditions. In this way, it is possible to analyze the contraction of Ulva colonies during the first winter, and their expansion, starting from a situation given by the model itself. The overall

seasonal evolution of *Ulva r.* has been summarized by computing the temporal evolution of *Ulva r.* total biomass, its maximum density and the area covered by macroalgae colonies. These three indices start increasing in March, when light and temperature conditions become favourable for Ulva growth. Macroalgae reach very high standing crops at the end of the spring, (12 kg ww/m^2), when they cover more than 4000 cells, with a total biomass of $15 \cdot 10^6$ kg ww. Productivity decreases in autumn, and during the winter ulva colonies cover a small area, with a biomass density greater than 0.1 kg/m^2 in less than 150 nodes.

The spatial distributions of biomass, at three significant stages of the evolution outlined above, are shown in Fig. 3. Ulva colonies spread quite easily in contiguous areas, where they find favourable conditions: see the difference between Fig. 3a, representing the initial situation, and Fig. 3b, which shows the spatial distribution at day 210, when biomass density is at its maximum in the first year. The colonization can be stopped or slowed down by the presence of a natural barrier, such as deep channels or large areas in which the conditions are adverse to the development. For instance, the channel between areas b and c, marked in Fig. 1, has not been invaded by macroalgae. After the winter decrease, which is noticeable in Fig. 3c, macroalgae start expanding again and reach the spatial distribution of Fig. 3d at day 210 of the second year, when their density is again at its maximum. This simulated spatial pattern is in reasonable agreement with that obtained from field data shown in Fig. 4, which was sampled in 1987 (Sfriso et al., 1989). The two spatial distributions look similar, even though the simulation has been run using an averaged meteoclimatic scenario; results could be improved by using actual data.

The spatial distribution of macroalgae within a colony depends on the intraspecific competition for nutrients. Biomass density is higher in the new colonies, and on the edge of the old ones, where the concentration of quota is maintained above the limiting threshold by the fluxes of nutrients from the surroundings. The edge of a colony acts as a barrier, which strongly decreases the nutrient concentration in the water that reaches its core. This description is supported by the distributions of NH_4^+, presented in Fig. 5a, and of internal nitrogen in Ulva (quota) presented in Fig. 5b, both taken at day 210 of the second year. Comparing figures Fig. 5a and Fig. 3d, it can be noted that the nutrient is supplied by the channels, where its concentration is higher, and is almost totally assimilated in the shallow areas where Ulva is present. The nitrogen taken up is stored as quota, whose value is much higher at the edge of the colonies than in their cores (Fig. 5b). This simulation suggests that the nitrogen supplied from the city of Venice is readily assimilated and, therefore, that sewage immissions could represent important sources of nutrients.

The dynamic of Ulva colonies outlined above can be followed by plotting the seasonal evolution along one of its sections, as has been done in Fig. 6 for section, A–A′, which crosses the areas labelled as *a*, *b*, *c*, *d*, in Fig. 1. Water depth along the section is reported at the top of the figures. We focused first on area *b*, because it presents the typical evolution pattern for shallow water. This zone is 1 m deep and, since it is surrounded by a

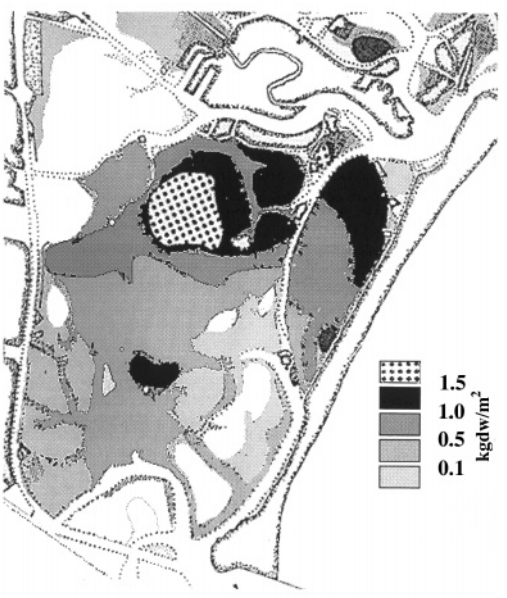

Fig. 4. Experimental distribution of Ulva in July 1987 as measured by Sfriso et al., 1989.

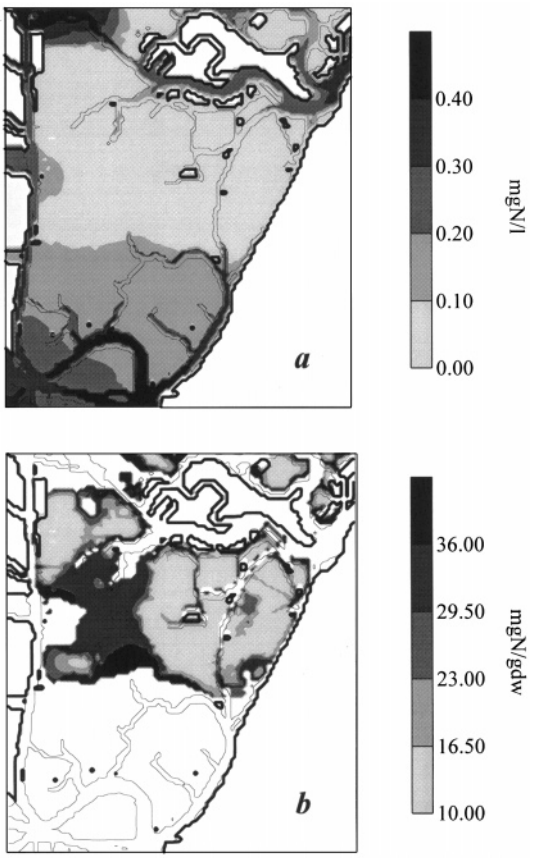

Fig. 5. Spatial distribution of nitrogen concentration (a) and quota (b) on day 210 of the second year of simulation

net of channels, a considerable flux of nutrients reaches it. At the beginning, (Fig. 6a, continuous line), the distribution of Ulva looks like a bell-shaped function: the peak then becomes broader and broader, until the higher growth rate at the edges causes a splitting of the initial distribution. Simulations show the same qualitative evolution in the other shallow areas, once their colonization starts. Colony *c* (1 m deep) reaches its maximum density later than *a* or *b*, which were invaded first. Moreover, standing crops in area *a* (2 m deep) are lower than in areas *b* and *c*. The evolution of the profiles during the second year, Fig. 6b, presents the same features, except for the initial condition, day 147, when there is no longer a single peak on area *b*, but a large colony, which has already split. Growth is much faster in area *d* (1 m deep) which is very close to the deepest channel and rich in nutrients; the biomass peak, which was barely noticeable at the end of the summer (day 252) increases up to 6 kg ww/m^2.

4.2. Dynamic of anoxic crisis

One of the main reasons for studying the dynamics of *Ulva r.* is the strong effect that this community exerts on the oxygen balance. DO is close to saturation along the major channels, and well above it, concurrently with algae blooms. Vertical discretization turns out to be very important in order to create a realistic simulation, because the vertical distribution of nutrients and DO, combined with the effects of shading and self shading, enable the reproduction of the dynamics of the anoxic crisis. Above a certain level of biomass, Ulva respiration and bacterial mineralization cause the depletion of DO, which becomes extremely low in the core of Ulva colonies, especially in the early morning. The crisis can persist in the bottom layers, where photosynthetic activity is reduced by nutrients depletion and self-shading. Since the lack of oxygen has a feedback effect on the rate of Ulva mortality, the oxygen demand for mineralization further increases. In these conditions, a local anoxia can cause a general dystrophic crisis, if reareation cannot restore the oxygen balance. As a consequence, the population of Ulva suddenly collapses. This is illustrated in Fig. 7, which shows the spatial distribution before, Fig. 7a, and just after the crisis. The phytoplanktonic pool can take advantage of the large amount of nutrients released by the decomposition of Ulva. In fact, phytoplankton, which behaves as a passive tracer, is less sensitive to local phenomena. This succession can be observed in the ecosystem and is correctly reproduced by the model, as discussed in Solidoro et al. (1997a).

4.3. Long term simulation under different scenarios of external forcings

Because of the intrinsically variable nature of real forcing functions, and the complexity of the ecosystem, an investigation of steady states would make little sense, even if the model eventually

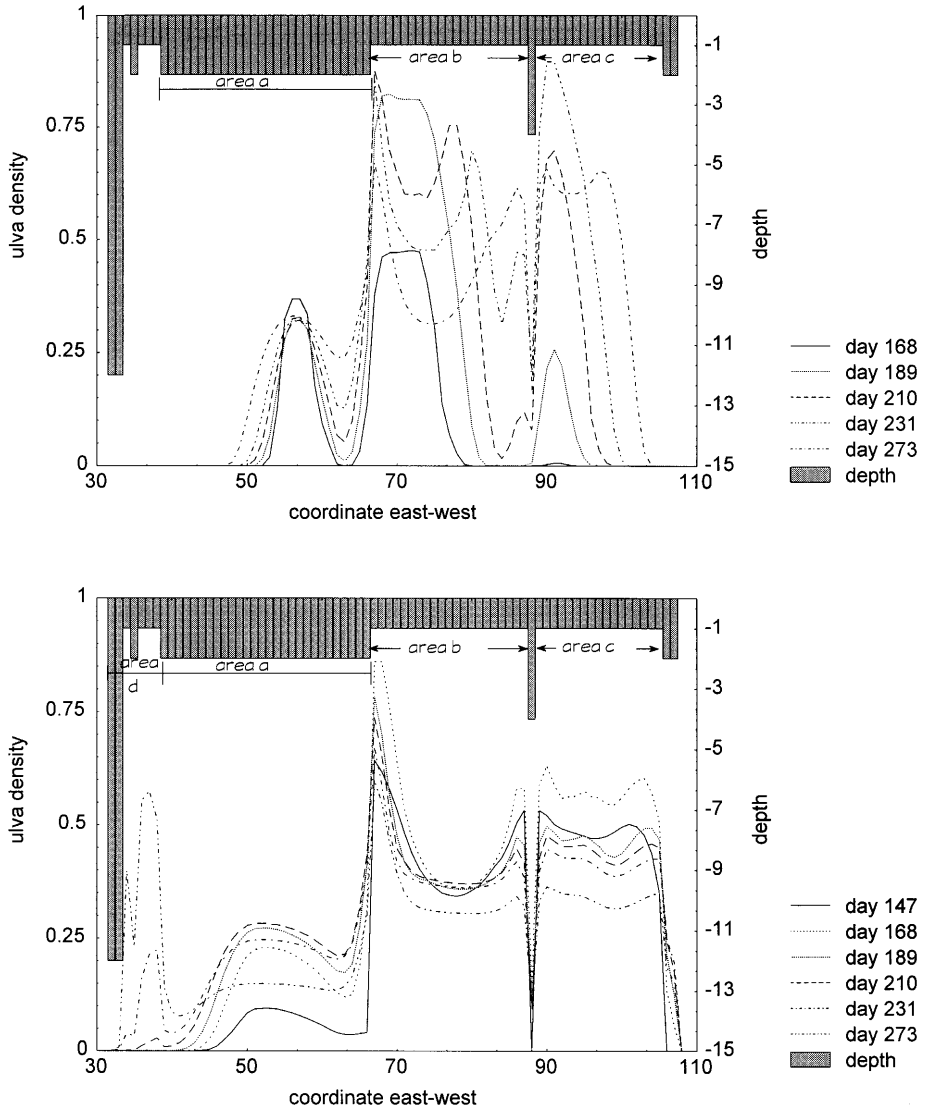

Fig. 6. Biomass evolution along the section A-A′ for the first (a) and the second (b) year of simulation. The depth is reported at the top of the figure.

reached a steady state evolution, when driven by the same forcings for many years. For this reason, we have focused our attention on the modality of expansion of Ulva colonies within a few years, trying to understand how different scenarios of loads of nutrients and light intensity affect the spatial distribution of *Ulva r.*

A reference scenario, called 'ref', has been obtained by running the model for three consecutive years, with the same forcings used in the above two year simulation. Another two scenarios have been obtained by running the model as above for two years, and then modifying the forcings for the third year: in the scenario labelled 'nutlim', nutrients loads have been halved, while in the one labelled 'lightlim', incident light intensity has been reduced by 30%. The results are compared in Fig. 8, which displays the spatial distribution of the

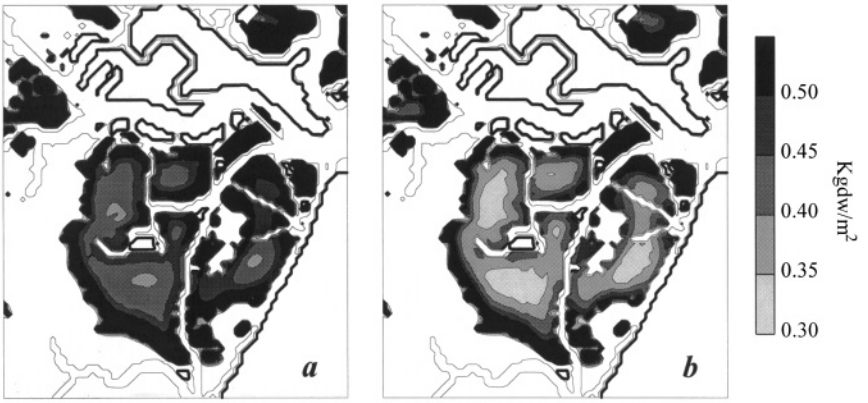

Fig. 7. Spatial distribution of Ulva density illustrating the decrement of density caused by an anoxic crisis: (a) refers to day 230 of the second year of simulation and (b) to day 235.

biomass on day 210 of the third year in the three cases, and in Fig. 9, which shows the number of grid cells occupied by Ulva colonies (a), and the evolution of the total biomass (b) during the third year.

The ref scenario shows a progressive colonization of the shallow areas (depth = 1, 2 m), as can be seen by comparing the distribution at day 210 of the second year, Fig. 3d, with Fig. 8a. This positive trend suggests that these forcings favour the expansion of the colonies; under continuation of these conditions the model indicates that all shallow areas would be covered by *Ulva r*. eventually.

The evolution of the colonies is strongly inhibited by a 30% reduction in the incident light: Ulva is absent in most areas which are over two meters deep, see Fig. 8b, because the level of irradiance reaching the bottom is not sufficient to sustain photosynthesis efficiently. Primary production is reduced also in areas which are over one meter deep, where Ulva density is lower, in comparison with the ref scenario. As a result, the trend of the colonization is no longer positive, as can be seen also in Fig. 9a and Fig. 9b, dotted line.

Halving the Nitrogen loads does not stop the colonization and does not cause a significant decrease in the total biomass, as we can see from Fig. 9a and 9b, dashed line. On the other hand, spatial distribution is sensitive to such a decrease in nitrogen availability. Fig. 8c shows that the density of biomass in area *a*, 2 m deep, is higher than in 'ref', despite the reduction in nitrogen. This somewhat unexpected evolution can be explained by the intraspecific competition between colonies in contiguous areas, *a* and *b*. Indeed, the lower the density of Ulva in area *b*, the less is the uptake of Nitrogen. For this reason, the amount of nutrient available in area *a* is higher, despite the reduction in input.

5. Conclusions

The model here discussed represents the first attempt at including the dynamic of macroalgae in a 3D water quality model of a coastal basin. The application to the lagoon of Venice is particularly interesting, because this ecosystem has been studied from many points of view, due to its peculiarity. The model has proved to be an effective tool for studying primary production in an eutrophic environment, where macro and microalgae are both present. A 3D model gives one the possibility to investigate the competition between the two communities of producers, as well as the intraspecific competition among and within Ulva colonies.

The two communities compete for the available nutrients, but their coexistence, or their extinction, is mainly regulated by the physical factors connected with light intensity, such as the depth

of the water column, and shading coefficients, and by their photosynthetic efficiencies. Vertical discretization turns out to be very important in improving the results, because it emphasizes the effects of the reareation as well as those of shading and self-shading.

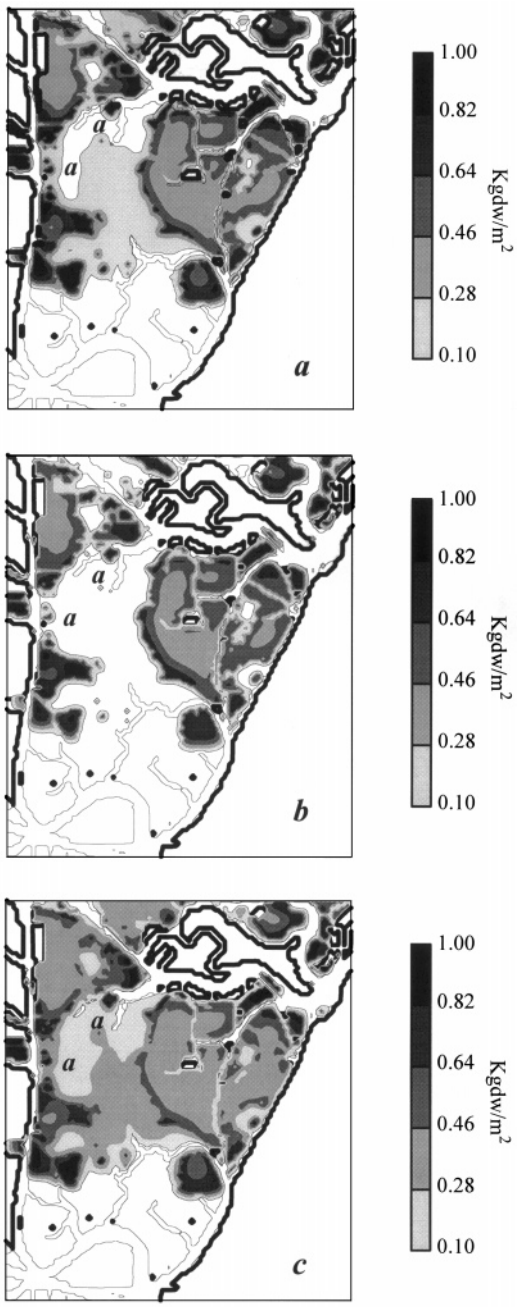

Fig. 8. Spatial distribution of Ulva density on day 210 of the third year of simulation for the three different scenario of forcing function (a) reference; (b) lightlim; (c) nutlim.

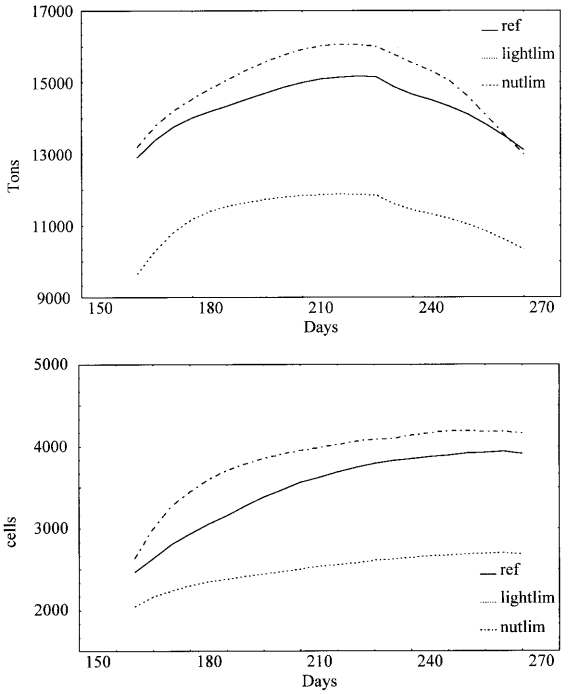

Fig. 9. Number of grid cells occupied by Ulva (a) and total biomass computed all over the area covered by the model (b) for the three different scenario of forcing functions.

The simulations here presented show that Ulva colonies survive only in shallow areas and that the colonization of Ulva is slowed down by natural barriers, such as deep channels; whereas the distribution of phytoplankton is not correlated with the bathimetry. The simulated spatial patterns are in reasonable agreement with those obtained from field data. The dynamic of anoxic crises is also correctly reproduced.

The density distribution of Ulva is mainly determined by the availability of nutrients and, therefore, the density is higher in areas closest to the main channels. Within a colony, the intraspecific competition for nutrients gives rise to a typical spatial distribution: biomass density is higher in the new colonies and on the edge of the old ones.

Even though, at this stage, the model cannot be used as a predictive tool, it can give useful qualitative indications about the long term dynamic of the ecosystem, under different scenarios of meteorological conditions and input of nutrients. The results, presented in Section 4, show that the effects of a consistent reduction in input are counterintuitive and difficult to analyze. This confirms the importance of taking into account the interaction between primary production and transport phenomena.

References

Bendoricchio, G., Coffaro, G., Di Luzio, M., 1993. Modelling the photosynthetic efficiency for *Ulva rigida* growth. Ecological Modelling 67, 221–232.

Bendoricchio, G., Coffaro, G., De Marchi, C., 1994. A Trophic Model for Ulva rigida in the Lagoon of Venice. Ecological Modelling 75/76, 485–496.

Bertonati, M., Dejak, C., Mazzei, I.L., Pecenik, G., 1987. Eutrophication model of the Venice Lagoon: statistical treatment of in situ measurement of phytoplankton growth parameters. Ecological Modelling 37, 103–130.

Cohen, I., Neori, A., 1991. *Ulva lactuca* biofilters for marine fishpond effluents. Bot. Mar. 34, 475–482.

CRTSF Comissione tecnico-scientifica di controllo sull'impatto della centrale termica ENEL di Fusina. Venice. Technical Report, 1989.

CRTSF, Comissione tecnico-scientifica di controllo sull'impatto della centrale termica ENEL di Fusina. Venice. Technical Report, 1994.

CVN, Consorzio Venezia Nuova, 1993, Valutazione della Quantita' di Nutrienti Scaricati in Laguna. Technical Report.

Dejak, C., Pecenik, G., 1987. Special issue: Venice lagoon. Ecological Modelling 37 (1/2), 1–101.

Dejak, C., Mazzei, I.L., Meregalli, L., Pecenik, G., 1987a. Development of a mathematical eutrophication model of the lagoon of Venice. Ecological Modelling 37, 21–45.

Dejak, C., Mazzei, L.I., Messina, E., Pecenik, G., 1987b. A two-dimensional diffusion model of the Venice Lagoon and relative open boundaries condition. Ecological Modelling 37, 21–45.

Dejak, C., Franco, D., Pastres, R., Pecenik, G., 1990. A 3D eutrophication–diffusion model of the Venice Lagoon: Some Application. In Cheng, R.T. (Ed.), Residual Currents and Long-term Transport. Coastal and Estuarine Studies, Vol. 38. Springer Verlag, Berlin. pp. 526–538

Dejak, C., Franco, D., Pastres, R., Pecenik, G., Solidoro, C., 1992. Thermal exchanges at air–water interfacies and reproduction of temperature vertical profiles in water columns. J. Mar. Sys. 3, 465–476.

Dejak, C., Franco, D., Pastres, R., Pecenik, G., Polenghi, I., Solidoro, C., 1995. 3D modelling of water quality transport process with time and space varying diffusivity tensors. In: Proceedings of IUTAM 1995. University of Western Australia, Perth, September 1995.

Fujita, R.M., 1985. The role of nitrogen status in regulating transient ammonium uptake and nitrogen storage by macroalgae. J. Exp. Mar. Biol. Ecol. 92, 283–301.

Joergensen, S.E., 1988. Fundamentals of Ecological Modelling, Elsevier, Amsterdam.

Menesguem, A., Salomon, J. 1987. Eutrophication modeling as a tools for fighting against Ulva coastal mass blooms. In: Schrefler, B.A. (Ed.), Computer modelling in ocean engineering. Balkema, Rotterdam.

Pastres, R., Franco, D., Pecenik, G., Solidoro, C., Dejak, C., 1995. Using parallel computers in environmental modelling: a working example. Ecological Modelling 80 (1), 69–86.

Pastres, R., Franco, D., Pecenik, G., Solidoro, C., Dejak, C., 1997. Local sensitivity analysis of a distributed parameter water quality model. Rel. Eng. Sys. Safety, in press.

Pecenik, G., Solidoro, C., Franco Davide, Dejak, C., Franco Daniel, 1991. Modelling the 'macroalgae' growth: a eutrophic diffusion macromodel of the Venice Lagoon. S.I.T.E. Atti, 12.

Redfield, A.C., 1934. On the proportions of organic derivates in sea water and their relation to the composition of plankton. James Johnston Memorial Volume. Liverpool University Press, Liverpool, pp. 176–192.

Sfriso, A., 1987. Flora and vertical distribution of macroalgae in the lagoon of Venice: a comparison with previous studies. Giornale Botanico Italiano 121, 69–85.

Sfriso, A., Marcomini, A., Pavoni, B., 1987. Relationship between macroalgal biomass and nutrient concentrations in a hypertrophic area of the Venice Lagoon. Mar. Environ. Res. 22, 297–312.

Sfriso, A., Pavoni, B., Marcomini, A., 1989. Macroalgae and phytoplankton standing crops in the central Venice Lagoon: primary production and nutrient balance. Sci. Total Environ. 80, 139–159.

Solidoro, C., Dejak, C., Franco, D., Pastres, R., Pecenik, G., 1995. A model for macroalgae and phytoplankton growth in the Venice Lagoon. Int. Environ. 21 (5), 619–626.

Solidoro, C., Brando, E.V., Dejak, C., Franco D., Pastres R., Pecenik, G., 1996a. Remote sensing as a tool for 3D model of ecosystem: an application to lagoon of Venice. In: Zannetti, P. (Ed.), Computer Techniques in Environmental Studies VI. Springer Verlag, Berlin; Computational Mechanics, Southampton, pp. 427–436.

Solidoro, C., Pastres, R., Franco, D., Pecenik, G., Dejak, C., 1996b. Sensitivity analysis of an eutrophication model for shallow water environment colonised by *Ulva rigida*. Ann. Chim., J. Env. An. Chem. 86, 677–684.

Solidoro, C., Brando, V.E., Dejak, C., Franco, D., Pastres, R., Pecenik, G., 1997a. Simulation of seasonal evolution of macroalgae in the Lagoon of Venice. Environ. Modelling Asses., in press.

Solidoro, C., Dejak, C., Franco, D., Pastres, R., Pecenik, G., 1997b. Modelling macroalgae (*Ulva rigida*) in the Venice Lagoon: model structure identification and first parameters estimation. Ecological Modelling, 94, 191–206.

Voinov, A.A., Tonkikh, A.P., 1987. Qualitative model of eutrophication in macrophyte lakes. Ecological Modelling 35, 211–226.